JOURNAL OF SOLID STATE CHEMISTRY 83, 8–19 (1989)

Crystal Chemistry of Hexaaluminates: β-Alumina and Magnetoplumbite Structures

N. IYI, S. TAKEKAWA, AND S. KIMURA

National Institute for Research in Inorganic Materials, Namiki 1-1, Tsukuba-shi, Ibaraki 305, Japan

Received March 27, 1989; in revised form June 12, 1989

Hexagonal aluminates are known to have a layer structure composed of spinel blocks and conduction layers which are stacked alternately. The structural parameters are influenced by the large cations in the conduction layer. Two typical types of hexagonal aluminates, β-alumina and magnetoplumbite, are studied and reviewed from this point of view. The conclusions are that the structure type of hexaaluminates is determined by the charge and radius of the large cations in the conduction layer, and that the conduction layer thickness decreases as the radii of the large cations in the conduction layer decreases and as the population increases. The spinel block thickness increases according to the increase in the amount of Al^{3+} defect within the spinel block.

1. Introduction

Hexagonal aluminates having a β-alumina, magnetoplumbite, or related layer structure have been commonly referred to as hexaaluminates. Na β-alumina is best known for its superior ion conductivity. It has been revealed that not only monovalent cations but also large di- and trivalent cations can be incorporated into hexaaluminate structures (*1–4*). The application of these hexaaluminates is not limited to ion conduction. Use as the host material for fluorescence (*5–10*), laser processes (*11*), nuclear waste disposal (*12, 13*), and high-temperature combustion catalysis (*14*) has also been proposed recently. The chemical formula and structure type were discussed and summarized by Stevels and Schrama-de Pauw in 1976 (*15*). Since then structural and chemical knowledge of this group of compounds has been accumulated; nevertheless, the crystal chemistry of this interesting structure group has not been discussed comprehensively so far. Only recently has some attention been paid to this matter (*16, 17*).

The purpose of this paper is to clarify the factors which have an effect on the structure type and the structure parameters of two typical hexaaluminates, β-alumina and magnetoplumbite. β″-Aluminas are not considered in this paper.

β-Alumina and magnetoplumbite (MP) consist of "spinel blocks" and "conduction layers," which are stacked alternately to form a sort of layer structure. Spinel blocks are composed only of Al^{3+} and O^{2-} ions, having the same rigid structure as spinel. Large cations such as Na^+, K^+, Sr^{2+}, and La^{3+} are usually accommodated in the spacious conduction layer which has a mirror symmetry plane. The major difference between β-alumina and MP lies in the con-

0022-4596/89 $3.00

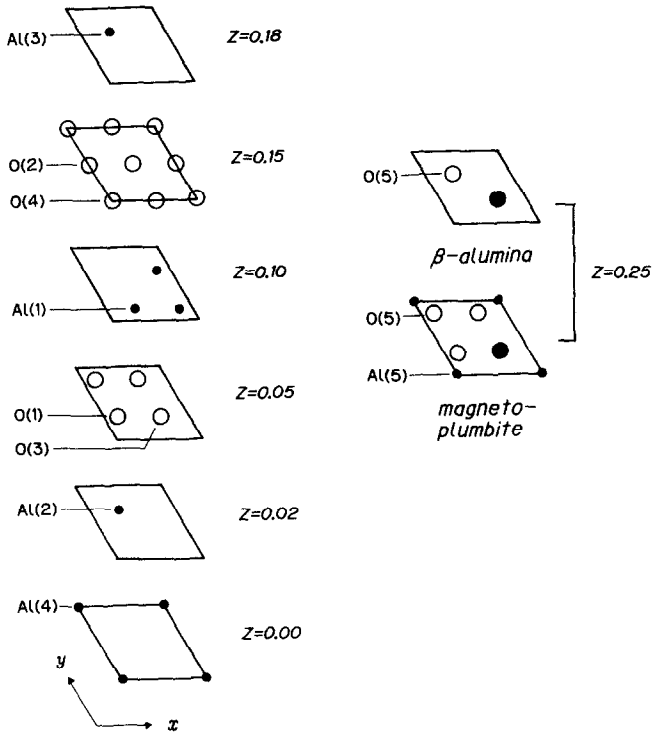

FIG. 1. Nomenclature of the atomic positions in β-alumina and magnetoplumbite structures. Atoms are shown layer by layer. The mirror planes are at $z = 0.25, 0.75$ and the centers of symmetry are at $(\frac{1}{2}, \frac{1}{2}, 0)$ and $(\frac{1}{2}, \frac{1}{2}, \frac{1}{2})$.

tents and arrangement of the ions within the conduction layer. Figure 1 shows these structures layer by layer. The nomenclature of each atom shown in this figure will be used throughout this paper.

From the viewpoint of composition as well as of structure, defect mechanism in the hexaaluminate structure is important. The chemical formulae of β-alumina and MP are ideally expressed as $MAl_{11}O_{12}$ and $MAl_{12}O_{19}$ (M: large cation), respectively. These stoichiometric expressions are limited to a few MP compounds, for example, $CaAl_{12}O_{19}$ (*18, 19*) and $SrAl_{12}O_{19}$ (*20*). Nonstoichiometric composition has been observed for almost all β-aluminas and trivalent lanthanoid-ion-containing MP compounds (*21, 22*). Na β-alumina contains excess Na^+ ions on the mirror plane and has been represented as $Na_{1+x}Al_{11}O_{17+x/2}$ ($x \approx 0.25$). For charge compensation of excess cations, a complex Frenkel defect (or Reidinger defect) mechanism was proposed on the basis of neutron diffraction data (*23*) and supported by energy calculations (*24*). According to this mechanism, a pair of interstitial Al^{3+} ions which have migrated from spinel blocks by the Frenkel defect mechanism are bridged by an interstitial oxygen ion on the mirror plane. Thus the charge due to excess cations on the mirror plane is compensated for by the interstitial oxygen ions formed by this complex defect mechanism in the case of nondoped hexaaluminates. Other mechanisms, such as a Schottky-type Al^{3+} deficiency, have not been proved. Hexaaluminates can contain Mg^{2+} or Li^+ as a dopant

in the spinel block. In this case, excess cations are charge-compensated by the doped ions (Mg^{2+} or Li^{+}) at the Al(2) site. In short, the Reidinger defect mechanism operates in the nondoped hexaalumiantes; on the other hand, the excess cation charge is compensated for by the mono- or divalent dopants in the doped hexaaluminates.

From Fig. 1, one would expect that the charge, ionic radius, and number of large cations in the conduction layer would have an important effect on the structure of hexaaluminates. These influences will be investigated in the following order:

(a) the effect of ionic radius and charge on the structure type;

(b) the effect of ionic radius on the conduction layer dimension;

(c) the effect of the cation population (in the conduction layer) on the dimension of the conduction layer.

The influence of the Al^{3+} defects within the spinel blocks on the spinel block size will also be discussed. In the last section, because the chemical formulae of the hexaaluminates are closely related to the structure type and defect mechanism, the question of the chemical formulae of the hexaaluminates will be addressed.

2. Effect of Ionic Radius and Charge on Structure Type

The structure type of the hexaaluminates in relation to the ionic radii and charge of the cation in the conduction layer is summarized in Fig. 2 on the basis of the data published so far for monovalent cations (*25–28*); for divalent cations (*18–20* and *29–32*); and for trivalent cations (*21, 33–38*). Only the nondoped hexaaluminates will be discussed in this section, and, because stable phases are the major concern in this case, only the compounds which can be synthesized directly from the component oxides are referred to when structure

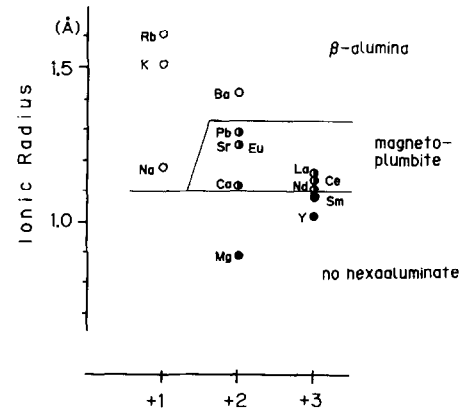

FIG. 2. Schematic depiction of the fields of β-alumina and magnetoplumbite structures for the MO_x–Al_2O_3 system.

type is discussed. The ionic radii were taken from Shannon and Prewitt (*39*) and those for 8-coordination are used throughout this paper.

Ionic Radii and Structure Type

Hexaaluminates containing divalent cations in the conduction layer change their structure types according to their ionic radii. Small divalent cations such as Mg^{2+} cannot form a hexaaluminate compound. Larger divalent cations form MP-type hexaaluminates. In the case of the divalent cations larger than 1.33 Å (e.g., Ba^{2+} ion: 1.42 Å), the β-alumina structure is preferred. The upper limit of 1.33 Å for the MP type can be explained as follows: In MP structure a large cation is coordinated by 12 oxygen ions: six O(2) ions at the 12*k* sites (above and below the large cation) and six O(5) ions at the 6*h* sites on the same mirror plane (Fig. 1). In Fig. 3, bond lengths *M*–O(2) and *M*–O(5) are plotted vs ionic radii. The *M*–O(5) length shows little increase, which indicates the rigid face-sharing connection between Al octahedra in the conduction layer; on the other hand, the *M*–O(2) length increases steeply and linearly in accordance with the increase in

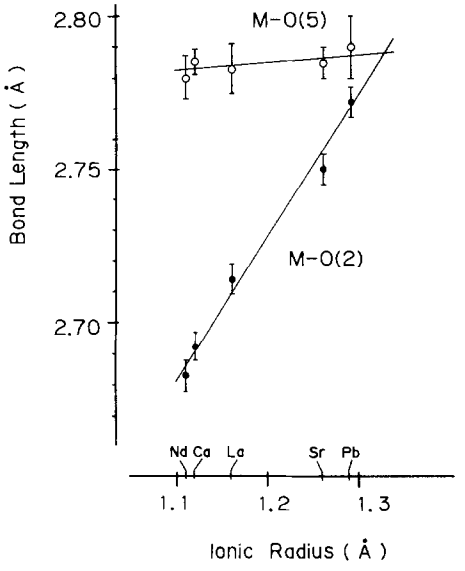

FIG. 3. Change of two M–O lengths as a function of ionic radii of the large cations (M) on the mirror plane (magnetoplumbite structure).

the large cation size. This means that a large cation is in full contact with O(2), not with O(5). The difference between the lengths of M–O(2) and M–O(5) decreases as the cation size increases. As the M–O(5) length cannot change due to the repulsion between O(5) ions, the point where the lengths of M–O(5) and M–O(2) become equal can be expected to be the upper limit of the MP structure. This corresponds to an ionic radius of 1.33 Å (Fig. 3).

The cations having radii less than 1.33 Å can enter either the β-alumina or the MP structure. In this case, other factors such as ionic charge and extent of defect must be taken into consideration. The chemical formulae of β-alumina ($M\mathrm{Al}_{11}\mathrm{O}_{17}$) and MP ($M\mathrm{Al}_{12}\mathrm{O}_{19}$) differ slightly. In the case of stoichiometric β-alumina, the chemical formula requires a monovalent cation for M to maintain charge neutrality; in the case of stoichiometric MP, the stoichiometric chemical formula requires a divalent cation for M. Thus, the amount of defect expected to be created differs according to the structure type. For example, trivalent cations, such as La^{3+}, cannot enter the M site of MP ($M\mathrm{Al}_{12}\mathrm{O}_{19}$) without creating some defects to attain the charge balance. In fact, lanthanum hexaaluminate was reported to have complex defects at several Al and lanthanum sites (*21, 22*). If the ionic radius conditions are met, cations might be accommodated in the less defective structure.

It is already known that some Mg-doped hexaaluminates have structures different from nondoped hexaaluminates (MP-type $\mathrm{SrAl}_{12}\mathrm{O}_{19}$ and β-alumina-type $\mathrm{SrMgAl}_{10}\mathrm{O}_{17}$) (*15*). The structure field of the Mg-doped M^{2+} hexaaluminates is shown in Ref. (*15*). The tendency to have less defective structure makes the MP structure field narrow for Mg-doped M^{2+} hexaaluminates, while the MP-type region is extended (*40*) to the smaller Gd^{3+} ion for Mg-doped Ln^{3+} hexaaluminates (Ln : lanthanoid) for the same reason (*41*). In the case of the hexaalumiantes containing monovalent cations, the MP structure cannot be formed without creating oxygen defects in the spinel block because there is no room for excess monovalent cations to be incorporated into the congested MP conduction layer for maintaining charge neutrality. Schottky-type defect of oxygen in the spinel block is not known as the defect mode for hexaaluminates structure, so this may not occur. The preference for the less defective structure is also an important factor in considering the structure type of hexaaluminates. Another important factor—charge—will be discussed in the next section.

Charge and Structure Type

It was postulated by Pauling(*42*) that the formal valence of an anion is close to the bond strength received from the adjacent cations in stable compounds ("the electrostatic valence rule"). So far the Mg^{2+} site

TABLE I

SITE ENERGY OF STOICHIOMETRIC β-ALUMINA[a]

Atom	Site	Charge (e)	Potential (e^2/Å)
K	2*d*	+1	−1.01
Al(1)	12*k*	+3	−2.42
Al(2)	4*f*	+3	−2.22
Al(3)	4*f*	+3	−2.74
Al(4)	2*a*	+3	−2.24
O(1)	12*k*	−2	+2.11
O(2)	12*k*	−2	+1.77
O(3)	4*f*	−2	+2.10
O(4)	4*e*	−2	+1.75
O(5)	2*c*	−2	+1.46

[a] Positional parameters of K β-alumina (*44*) were used for the calculation.

has been successfully interpreted by this rule in a Mg-doped β-alumina (*23*). By using this criterion, the charge of the large cation in the conduction layer required for the ideal structure can be estimated (*43*). The bridging oxygen ions are coordinated by two tetrahedral Al^{3+} ions and by three 9-coordinated large cations on the mirror plane. As the formal valence of oxygen is −2.0, the equation $2(3/4) + 3(y/9) = 2$ should be satisfied (y: ideal valence at the large cation site). Solving this equation, we obtain $y = +1.5$ as the ideal cation charge in the case of stoichiometric β-alumina. This implies that the cation charge in the conduction layer is not sufficient at the stoichiometric composition $MAl_{11}O_{17}$ (*43*). In fact, (electrostatic) site energy calculations for stoichiometric β-alumina revealed that the site potential at the bridging oxygen O(5) is less than those of oxygen ions at other sites (Table I). Furthermore, low site potential was observed at the oxygen sites (O(2), O(4)) adjacent to the conduction layer. (Here, stoichiometric composition was assumed, and the Ewald method (*45–47*) was employed for energy calculation.) Stoichiometric β-alumina, $MAl_{11}O_{17}$, has been produced only by special synthetic routes (*48, 49*), and is considered to be an unstable phase. Low site potential of the oxygen site may be one of the reasons for accommodation of excess cations in the conduction slab. Wang *et al.* (*50*) have already explained the Mg^{2+} substitution at the Al(2) site from the viewpoint of electrostatic potential. This implies that Pauling's valence rule is closely related to electrostatic site potential. Incidentally, for the β-alumina structure, a divalent cation in one conduction layer exhibits a small excess positive charge, so it would contain more oxygen ions or it would contain defects of divalent cations in the conduction layer. Such a trend may favor Ba β-alumina formation.

On the other hand, the ideal charge of the large cation for a magnetoplumbite structure is assumed to be +2.4. For M^{2+} hexaaluminates, slightly more positive charge is needed, but there is no space to accommodate more cations. Thus, a typical fully occupied magnetoplumbite structure is formed. For the case of the hexaaluminates containing trivalent cations, the cation charge is so large that a reduction of the cation number in the conduction layer is needed. This trend satisfies the condition that Ln^{3+} hexaaluminates are formed. For monovalent cations, the MP structure is not expected because the positive charge is too small and the bridging oxygen would be underbonded.

In conclusion, the MP structure becomes favorable as the charge of the large cation on the mirror plane increases, and the β-alumina structure becomes more stable as the cation size increases.

3. Effect of Ionic Radius on Conduction Layer Size

It is known that the c value of lattice parameters becomes larger as the radius of the monovalent cation in the conduction layer increases (Kummer (*51*)). Further-

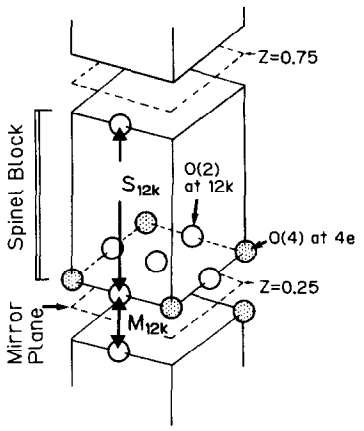

FIG. 4. Simplified hexaaluminate structure showing the thickness of the conduction layer M_{12k} and the thickness of the spinel block S_{12k}. Open circles represent O(2) at the 12*k* site and shaded circles are O(4) at the 4*e* site.

more, Newsam and Tofield (*52*) and Boilot *et al.* (*53*) described the tendency of the *c* parameter to decrease according to the increase in the cation population in the conduction layer. This strange phenomenon has also been reported in β''-aluminas (*54*), hexaferrites (*55*), and β-alumina-type gallates (*56*). However, this is not a general rule, as has already been pointed out. For example, $K_{1.3}$ and $K_{1.5}$ β-aluminas have been shown to have almost the same *c*-axis parameter of 22.73 Å (*57*). Other parameters than the *c*-axis length are necessary to describe the microscopic structural effects of cation radius and population.

Conduction Layer Thickness and Spinel Block Thickness

Large cations in the conduction layer are coordinated by six oxygens at the 12*k* sites (O(2) in this paper) just above and below the conduction layer in addition to three (in the case of β-alumina) or six (in the case of the MP structure) oxygen ions on the mirror plane (O(5) in this paper). Generally, the cation–oxygen distance is smaller for *M*–O(2) than for *M*–O(5), so O(2) ions will be more directly influenced by the change of cation species or population. The present authors (*57*) defined the distance between O(2) ions through the mirror plane as "the thickness of the conduction layer" (M_{12k}), and the inter-O(2) distance measured across the spinel block as "the thickness of the spinel block" (S_{12k}) as shown in Fig. 4. These parameters are related by the equation $c = 2 \times (M_{12k} + S_{12k})$.

The relation between ionic radius and M_{12k} will be discussed in the remainder of this section, and the relation between the cation population and M_{12k} will be discussed in the next section.

Conduction Layer Thickness and Ionic Radius

As the cation radius becomes larger, the distance M_{12k} should increase. In Fig. 5, this relationship is shown. The lower limit is 4.6 Å in the case of β-alumina (data from Refs. (*25, 31, 44, 58–60*)). The same trend was previously observed in the relation between the *c* parameter and the ionic radius of β-alumina (*28*). Below the 4.6-Å limit is

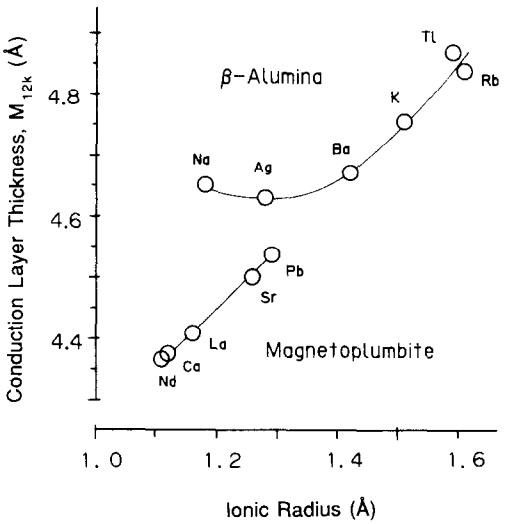

FIG. 5. Dependence of the conduction layer thickness M_{12k} on the ionic radius in β-alumina and magnetoplumbite structures.

TABLE II

COMPARISON OF THE PARAMETERS OF BRIDGING Al TETRAHEDRON AND CONDUCTION LAYER THICKNESS IN VARIOUS M^+ β-ALUMINAS

	Na-β	Ag-β	K-β	Tl-β^a	Tl-β^b	Rb-β
Ionic radius[c] (Å)	1.18	1.28	1.51	1.59	1.59	1.61
Angle β^d (°)	68.5	68.7	67.8	66.8	66.5	66.9
O(2)–Al(3) (Å)	1.768	1.762	1.775	1.774	1.784	1.782
O(5)–Al(3)[e] (Å)	1.677	1.673	1.707	1.720	1.723	1.719
M_{12k} (Å)	4.65	4.63	4.76	4.84	4.87	4.84

[a] Ref. (*58*).
[b] Ref. (*44*).
[c] Ionic radius of monovalent cation on the mirror plane.
[d] See Fig. 9. β = 180°, angle (O(2)–Al(3)–O(5)).
[e] If the O(5) ion was not situated at the 2*c* site (the ideal O(5) position), the 2*c* site was taken as the O(5) position.

the region of the MP structure. This lowest limit may be determined by the distance of Al–O–Al, which bridges the spinel blocks. The M_{12k} distance would ideally be 4.67 Å if the tetrahedral Al–O distance is assumed to be 1.752 Å (Bauer (*61*)). The dependence of M_{12k} length on the ionic radius was also observed in the MP structure despite this structure's appearing to have a more rigid frame than β-alumina (data from Refs. *18–21, 38*). As the ionic radius increases, M_{12k} becomes larger. In the MP structure, the octahedral Al–O–Al face-sharing connection is directly related to the M_{12k} value, which can be ideally calculated as 4.41 Å if the average octahedral Al–O distance is assumed to be 1.909 Å. These are only ideal values, but a general trend can be seen. In short, conduction layer thickness is largely determined by the coordination of bridging Al^{3+} ions and this length is modified by the ionic radii and population of large cations on the mirror plane.

It was pointed out by Verstegen and Stevels (*62*) that the axis ratio *c*/*a* was related to the structure type; i.e., beyond *c*/*a* = 3.98 lies the β-alumina region and below is the MP region. As there is little difference in the *a*-axes and as the difference in spinel block thicknesses between β-aluminas and MP compounds can be negligible, the axis ratio usually behaves in a way similar to that of M_{12k}. For this reason their empirical rule has proved to be a useful tool for distinguishing two types of hexaaluminates.

Table II shows the deformation of the Al(3) tetrahedron due to the ionic radii of the large cations on the mirror plane. As pointed out by Kodama and Muto (*59*), the length of the Al(3)–O(5) bond increases as the large cations in the conduction layer become bigger. In addition, the O(2)–Al(3)–O(5) angle and the Al(3)–O(2) length seem to increase (Fig. 6). The Al(3) tetrahedron elongates in the *c* direction as the ionic radii of large cations increase. This deformation leads directly to the increase in the conduction layer thickness M_{12k}.

4. Cation Population and Conduction Layer Thickness

The values of M_{12k} for $K_{1.30}$ β-alumina and $K_{1.50}$ β-alumina are 4.756 and 4.716 Å, respectively (*44, 57*). The contraction of the thickness of the conduction layer by 0.040 Å can be observed. Well-characterized Ag β-aluminas show the same tendency for M_{12k} (Fig. 7a). At 4 K, stoichiometric $AgAl_{11}O_{17}$ (*49*) has an M_{12k} of 4.68 Å; on the other hand, $Ag_{1.45}$ β-alumina (*64*),

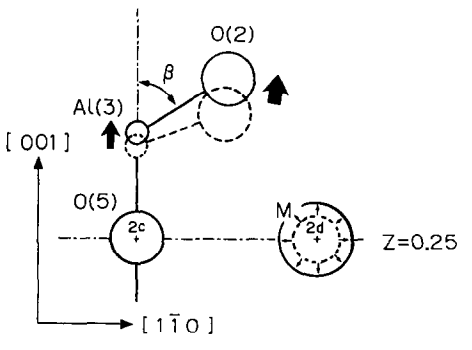

FIG. 6. The deformation of bridging Al tetrahedron due to the increase of ionic radius of the large cation in the conduction layer. O(2) and Al(3) migrate in the direction of the arrow as the ionic radius increases.

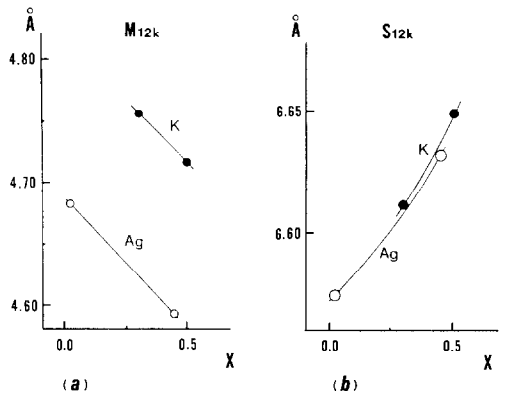

FIG. 7. Relation between excess cation content (x) per unit formula and (a) M_{12k} or (b) S_{12k} in the case of K β-aluminas and Ag β-aluminas (by Iyi *et al.* (*57*)).

with an excess of cations, has a smaller M_{12k} value of 4.60 Å. This relation is also true for $Ag_{1.0}$ β-alumina (*48*) and $Ag_{1.33}$ β-alumina (*60*) measured at room temperature. (Figure 7b shows the change in the spinel block thickness, which will be discussed in the next section.)

In nondoped β-aluminas, the number of excess large cations is directly related to the number of interstitial oxygen ions on the mirror plane due to the complex Frenkel-type defect (*23*). The contraction of the conduction layer thickness M_{12k} may be attributed to additional Al_i–O_i–Al_i (i: interstitial) connections due to this complex defect, which would pull the spinel blocks (Newsam and Tofield (*52*)). However, conduction layer contraction can also be seen in the defect-free β-aluminas. In Fig. 8, the M_{12k} values of Mg-doped K β-aluminas, together with nondoped values, are plotted vs cation number per unit cell (data of Refs. (*44*, *57*, *63*, and *65*) were used). There are no interstitial oxygens or Al^{3+} ions in the conduction layer of these Mg-doped compounds. Nevertheless, the tendency of M_{12k} contraction can be observed as shown in Fig. 8. On the basis of these facts, it may be possible to say that the cation population itself influences the M_{12k} distance.

Another example of this effect is found in barium hexaaluminates. Ba β(II)-alumina (or Ba hexaaluminate phase II) was revealed to have perfect and defect conduction layers (*66*, *67*). The perfect layer contains 1.0 Ba^{2+} ion per layer, and the M_{12k} can be calculated for this layer. The M_{12k} of Ba β-alumina (*31*) and Ba · Mg β-alumina (*63*), as well as that of Ba β(II), are plotted vs Ba content in Fig. 9. The result agrees well with the above assumption.

Despite many observations on the relation between cation population and c parameter, sufficient explanations have not been given so far. The increase of Al_i–O_i–Al_i bonding has sometimes been attributed to the decrease in c parameter (*52*) and sometimes to the increase in c parameter (*56*). The deformation of the bridging Al tetrahedron is shown in Table III and depicted in Fig. 10 for the series of K β-aluminas. The flattening of Al(3) tetrahedron due to the increase in cation population can be observed. This deformation leads directly to the decrease in M_{12k}. Similar changes can be seen in Ba β-alumina compounds: angle β = 68.8° and Al(3)–O(5) bond length = 1.699 Å for $Ba_{0.75}Al_{11}O_{17.25}$ (*31*); on the

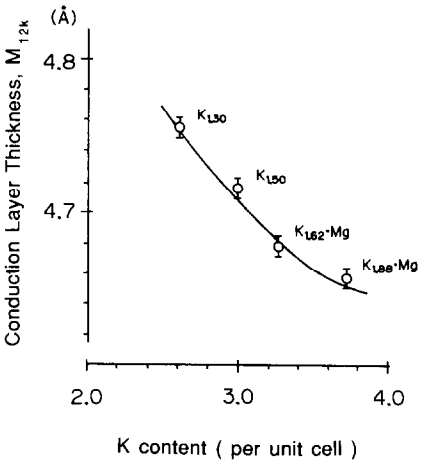

FIG. 8. Relation between the conduction layer thickness M_{12k} and K content in nondoped and Mg-doped K β-aluminas.

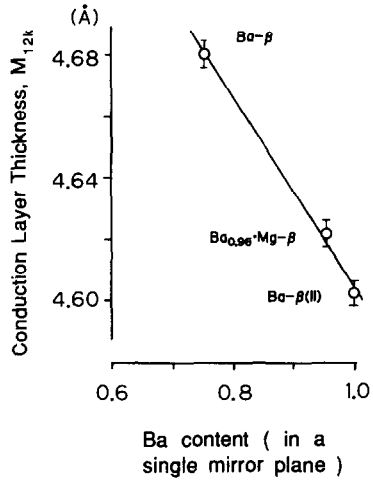

FIG. 9. The conduction layer thickness M_{12k} and Ba content in Ba β-aluminas. For Ba β(II)-aluminate, the fully occupied conduction layer was considered.

other hand, $\beta = 70.4°$ and bond length = 1.718 Å for $Ba_{0.956} \cdot Mg$ β-alumina (*63*). This deformation of the Al(3) tetrahedron is different from that due to the ionic radius (cf. Fig. 6). The cause of the Al tetrahedron deformation can be explained as follows: As the number of large cations increases in the conduction layer, positive charge concentrates on the mirror plane and repulsion among these cations becomes greater. To ease this repulsion, the negatively charged oxygen ions adjacent to the conduction

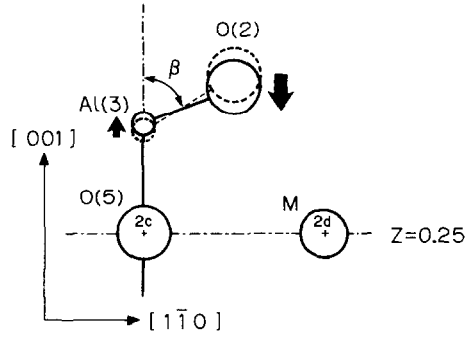

FIG. 10. The deformation of bridging Al tetrahedron due to the increase in cation content in the conduction layer. O(2) and Al(3) migrate in the direction of the arrow, owing to the increase in the cation (M) population.

TABLE III

COMPARISON OF THE PARAMETERS OF BRIDGING Al TETRAHEDRON AND CONDUCTION LAYER THICKNESS IN β-ALUMINAS WITH VARIOUS K CONTENTS

	$K_{1.30}$	$K_{1.50}$	$K_{1.62}$	$K_{1.88}$
Angle β[a] (°)	67.8	68.7	69.0	70.3
O(2)–Al(3) (Å)	1.775	1.769	1.759	1.766
O(5)–Al(3)[b] (Å)	1.707	1.715	1.710	1.733
z(O(2)–Al(3))[c] (Å)	0.671	0.642	0.629	0.596
M_{12k} (Å)	4.76	4.71	4.68	4.66

[a] See Fig. 9. β = 180°, angle (O(2)–Al(3)–O(5)).

[b] If the O(5) ion was not situated at the 2*c* site (the ideal O(5) position), the 2*c* site was taken as the O(5) position.

[c] The difference in z-coordinates between O(2) and Al(3) sites.

plane (O(2)) migrate toward the mirror plane between these large cations, which makes the spinel blocks both above and below the conduction layer move closer.

For the MP system, the data are insufficient to discuss this matter. However, contraction of M_{12k} seems to take place. For instance, Mg^{2+}-doped La hexaaluminate (1.92 La^{3+} per unit cell) (*11*) shows 4.36 Å for M_{12k}, and La hexaalumiante (1.65 La^{3+} per unit cell) (*38*) shows 4.41 Å. This fact suggests a similar influence of the population. Further structure data are needed to prove this effect in the case of MP.

Thus, the conduction layer thickness M_{12k} shows monotonic decrease as cation population increases, but, in the case of β-alumina, the behavior of M_{12k} near the lowest limit 4.6 Å remains unclear due to lack of data. Other factors such as distribution of the cations on the mirror plane may have an effect on M_{12k}, but there are not enough data to estimate the degree of contribution.

5. Frenkel Defects and Spinel Block Thickness

As shown in Fig. 7b, the distance S_{12k} for $K_{1.30}$ β-alumina is 6.611 Å and that for $K_{1.50}$

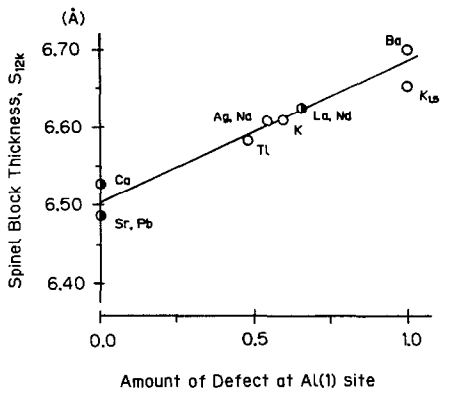

FIG. 11. Change in the spinel block thickness S_{12k} as a function of the amount of defect in the Al(1) site. The number of defects is given per unit cell (total number of Al(1) per unit cell = 12.0).

β-alumina is as large as 6.650 Å. The contraction of M_{12k} and enlargement of S_{12k} (owing to the excess potassium ions on the mirror plane) compensate for each other resulting in little difference between the c parameters (Fig. 7a and 7b). The increase in S_{12k} can be attributed to the concentration of Al^{3+} defect in the spinel block. This is also the case with Ag β-alumina, as already shown in Fig. 7a and 7b. Despite the variation in c parameters according to the cation species, the values of S_{12k} of nondoped M^+ β-alumina compounds which have about 30% excess cations are confined to the range 6.59–6.61 Å. The values of S_{12k} are plotted vs Al^{3+} vacancy in the spinel block in Fig. 11 for both types of hexaaluminates. The values S_{12k} of Ca hexaaluminate (MP structure) and $K_{1.5}$ β-alumina deviate a little; however, the increase in the spinel block thickness due to Al^{3+} vacancy is indicated. This is because the defects of Al^{3+} in the spinel block, which are equivalent to adding negative charges to this site, drive away the neighboring oxygen anions.

In conclusion, the structure type (β-alumina or MP) of hexaaluminates is determined by the charge and the radius of the cation in the conduction layer. The conduction layer thickness M_{12k} decreases as the radii of the large cations in the conduction layer decrease and as the population increases. The spinel block thickness S_{12k} increases according to the increase in the amount of Al^{3+} defect within the spinel block. As has been shown, the M_{12k} and S_{12k} changes can be explained by the microscopic structural change or deformation of the Al tetrahedron. The merit of using these parameters is that they are directly connected to the c parameter.

Recently, NaNd hexaaluminate (mixed-cation hexaaluminate) was revealed to have two different types of conduction layers (β-alumina type and MP type) which are stacked alternately in the c direction (*68*). For this interesting hexaaluminate, conduction layer thickness and spinel block thickness can be calculated. "M_{12k}" is 4.69 Å for the β-alumina-type conduction layer, that for the MP type conduction layer is 4.32 Å, and "S_{12k}" is 6.62 Å. These values are consistent with the data described above. Furthermore the thickness of spinel block suggests a small number of Al^{3+} vacancies, a little less Na^+ than Na β-alumina content (*25*), and a little more Nd^{3+} than Nd hexaaluminate content (*38*). These facts support the assumption that the dimension of the conduction layer is strongly influenced by the large cations in the manner described above, and indicate that the dimension of the conduction layer is retained even in such a mixed-cation hexaaluminate system.

6. Chemical Formulae of Hexaaluminates

The chemical formulae of hexaaluminate compounds are closely related to the type of the structure, so it is misleading to use conventional formulae such as $LaAl_{11}O_{18}$ and $BaAl_{12}O_{19}$. Derivatives of β-alumina should be represented in the form $M_{1+x}Al_{11+y}O_{17+z}$, those of MP in the form $M_{1-x}Al_{12-y}O_{19-z}$. The variables x, y, z differ

from case to case, but in most cases are less than 0.5. Thus, it is easy to grasp the structure type by the chemical formula. For example, M^+-containing hexaaluminates are expressed as $M_{1+x}Al_{11}O_{17+x/2}$. In this case, x is known to be about 0.25 for the directly synthesized compounds. The implications of this formula are as follows: (a) the fundamental structure is the β-alumina type; (b) the composition in a unit cell can be expressed by a multiple of this formula; (c) excess monovalent cations are incorporated into the structure; (d) Schottky-type defects of Al^{3+} may not occur in this structure; and (e) excess positive charge due to the cations is compensated for by the excess oxygen. For the hexaaluminates containing divalent cations such as Ca^{2+}, Sr^{2+}, Pb^{2+}, the chemical formula is $MAl_{12}O_{19}$. In the case of Ba^{2+}, two types of compounds are already recognized and well characterized (*31, 32, 66*). So-called phase I, Ba β-alumina, can be expressed as $Ba_{0.75}Al_{11}O_{17.25}$, and so-called phase II as $Ba_{2.33}Al_{21.33}O_{34.33}$. (As for Ba β-alumina, $Ba_{0.79}Al_{10.9}O_{17.14}$ was proposed (*31*) but later revised to $Ba_{0.75}Al_{11.0}O_{17.25}$ (*69*). This result is in accordance with Ref. (32).) Other possible expressions are $BaO \cdot 7.32Al_2O_3$ and $BaO \cdot 4.55Al_2O_3$ (*1, 2*), respectively. The latter compositional formulae only represent empirical ratio of the elements. The M^{3+} hexaaluminates have the MP structure, so the formula should be $Ln_{1-x}Al_{12-y}O_{19-z}$ (Ln: trivalent lanthanoid elements, z: $\{3(x + y) - 1\}/2$). As Stevels (*10*) and the present authors (*21*) have proposed slightly different values for x, y, and solid solution range, further evidence is needed to settle the question. For the present, it seems better to use the formula $Ln_{1-x}Al_{12-y}O_{19-z}$. Usually either $LnAl_{11}O_{18}$ or $Ln_2O_3 \cdot 11Al_2O_3$ has been used, but these formulae are utterly meaningless and misleading since these hexaaluminates are of the MP type, not the β-alumina type (*21, 22, 38*).

Acknowledgments

The authors are very grateful to Drs. Z. Inoue, and Y. Bando of our institute (NIRIM) for suggestions and technical help. Thanks are also due to Professor F. Kanamaru of Osaka University (Japan), and Dr. A. Petric of McMaster University (Canada) for helpful discussion.

References

1. F. Haberey, G. Oehlschlegel, and K. Sahl, *Ber. Dtsch. Keram. Ges.* **54,** 373 (1977).
2. S. Kimura, E. Bannai, and I. Shindo, *Mater. Res. Bull.* **17,** 209 (1982).
3. R. S. Roth and S. Hasko, *J. Amer. Ceram. Soc.* **41,** 146 (1958).
4. N. A. Toropov, V. P. Barzakovskii, V. V. Lapin, and N. N. Kurtseva, "Handbook of Phase Diagrams of Silicate Systems," Vol. 1, Jerusalem (1972).
5. G. Blasse and A. Bril, *Philips Res. Rep.* **23,** 201 (1968).
6. J. M. P. J. Verstegen, J. L. Sommerdijk, and J. G. Verriet, *J. Lumin.* **6,** 425 (1973).
7. A. L. N. Stevels and J. M. P. J. Verstegen, *J. Lumin.* **14,** 207 (1976).
8. A. L. N. Stevels, *J. Electrochem. Soc.* **125,** 588 (1978).
9. A. L. N. Stevels, *J. Lumin.* **17,** 121 (1978).
10. A. L. N. Stevels, *J. Lumin.* **20,** 99 (1979).
11. A. Kahn, A. M. Lejus, M. Madsac, J. Thery, D. Vivien, and J. C. Bernier, *J. Appl. Phys.* **52,** 6864 (1981).
12. P. E. D. Morgan and E. H. Cirlin, *J. Amer. Ceram. Soc.* **65,** C114 (1982).
13. C. M. Jantzen and R. R. Neurgaonkar, *Mater. Res. Bull.* **16,** 519 (1981).
14. M. Machida, K. Eguchi, and H. Arai, *Chem. Lett.* **1987,** 767 (1987).
15. A. L. N. Stevels and A. D. M. Schrama-de Pauw, *J. Electrochem. Soc.* **123,** 691 (1976).
16. N. Iyi, Ph.D. thesis, Osaka Univ., Japan (1986).
17. A. Petric, J. Kirchnerova, C. W. Bale, and A. D. Pelton, *in* "Proceedings of the Solid State Ionics Symposium, Boston, 1988."
18. K. Kato and H. Saalfeld, *N. Jb. Miner. Abh.* **109,** 192 (1968).
19. A. Utsunomiya, K. Tanaka, H. Morikawa, F. Marumo, and H. Kojima, *J. Solid State Chem.* **75,** 197 (1988).
20. A. J. Lindop, C. Matthews, and D. W. Goodwin, *Acta Crystallogr. Sect. B* **31,** 2940 (1975).
21. N. Iyi, Z. Inoue, S. Takekawa, and S. Kimura, *J. Solid State Chem.* **54,** 70 (1984).

22. M. GASPERIN, M. C. SAINE, A. KAHN, F. LAVILLE, AND A. M. LEJUS, *J. Solid State Chem.* **54,** 64 (1984).
23. W. L. ROTH, F. REIDINGER, AND S. LAPLACA, *in* "Superionic Conductors" (G. D. Mahan and W. L. Roth, Eds.), p. 223, Plenum, New York (1977).
24. J. C. WANG, *J. Chem. Phys.* **73,** 5786 (1980).
25. C. R. PETERS, M. BETTMAN, J. W. MOORE, AND M. D. GLICK, *Acta Crystallogr. Sect. B* **27,** 1826 (1971).
26. D. J. DYSON AND W. JOHNSON, *Trans. J. Brit. Ceram. Soc.* **72,** 49 (1973).
27. J. S. MOYA, E. CRIADO, AND S. DEAZA, *J. Mater. Sci.* **17,** 2213 (1982).
28. Y. F. Y. YAO AND J. T. KUMMER, *J. Inorg. Nucl. Chem.* **29,** 2453 (1967).
29. J. J. COMER, W. J. CROFT, M. KESTIGIAN, AND J. R. CARTER, *Mater. Res. Bull.* **2,** 293 (1967).
30. N. IYI, S. TAKEKAWA, AND S. KIMURA, unpublished data on Pb-hexaaluminate.
31. N. IYI, Z. INOUE, S. TAKEKAWA, AND S. KIMURA, *J. Solid State Chem.* **52,** 66 (1984).
32. F. P. F. VAN BERKEL, H. W. ZANDBERGEN, G. C. VERSHOOR, AND D. J. W. IJDO, *Acta Crystallogr. Sect. C* **40,** 1124 (1984).
33. M. MIZUNO, R. BERJOAN, J. P. COUTURES, AND M. FOEX, *Yogyo Kyokaishi* **82,** 631 (1974).
34. M. MIZUNO, R. BERJOAN, J. P. COUTURES, AND M. FOEX, *Yogyo Kyokaishi* **83,** 50 (1975).
35. M. MIZUNO, T. YAMADA, AND T. NOGUCHI, *Yogyo Kyokaishi* **85,** 374 (1977).
36. M. MIZUNO, T. YAMADA, AND T. NOGUCHI, *Yogyo Kyokaishi* **85,** 91 (1977).
37. J. P. COUTURES, *J. Amer. Ceram. Soc.* **68,** 105 (1985).
38. N. IYI, Z. INOUE, AND S. KIMURA, *J. Solid State Chem.* **54,** 123 (1984).
39. R. D. SHANNON AND C. T. PREWITT, *Acta Crystallogr. Sect. B* **25,** 925 (1969).
40. P. E. D. MORGAN AND J. A. MILES, *J. Amer. Ceram. Soc.* **69,** C-157 (1986).
41. J. LIEBERTZ, *Z. Kristallogr.* **166,** 297 (1984).
42. L. PAULING, "The Nature of the Chemical Bond," 3rd ed., Cornell Univ. Press, Ithaca, New York (1960).
43. A. R. WEST, *Mater. Res. Bull.* **14,** 441 (1979).
44. G. COLLIN, J. P. BOILOT, A. KAHN, J. THERY, AND R. COMES, *J. Solid State Chem.* **21,** 283 (1977).
45. C. KITTEL, "Introduction to Solid State Physics," Appendix A, 2nd ed., Wiley, New York (1953).
46. M. CATTI, *Acta Crystallogr. Sect. A* **34,** 974 (1978).
47. D. WILLIAMS, *Acta Crystallogr. Sect. A* **27,** 452 (1971).
48. J. B. BOILOT, PH. COLOMBAN, G. COLLIN, AND R. COMES, *J. Phys. Chem. Solids* **41,** 47 (1980).
49. J. M. NEWSAM AND B. C. TOFIELD, *J. Phys. C* **14,** 1545 (1981).
50. J. C. WANG, J. B. BATES, N. J. DUDNEY, AND H. ENGSTROM, *Solid State Ionics* **5,** 35 (1981).
51. J. T. KUMMER *in* "Progress in Solid State Chemistry" (Reiss and McCaldin, Eds.), Vol. 7, p. 141, Pergamon Press, New York (1972).
52. J. M. NEWSAM AND B. C. TOFIELD, *Solid State Ionics* **5,** 59 (1981).
53. J. B. BOILOT, G. COLLIN, PH. COLOMBAN, AND R. COMES, *Solid State Ionics* **5,** 157 (1981).
54. F. HARBACH, *J. Mater. Sci.* **18,** 2437 (1983).
55. G. J. DUDLEY AND B. C. H. STEELE, *J. Mater. Sci.* **13,** 1267 (1978).
56. T. TSURUMI, H. IKAWA, K. URABE, AND S. UDAGAWA, *Yogyo Kyokaishi* **91,** 553 (1983).
57. N. IYI, Z. INOUE, AND S. KIMURA, *J. Solid State Chem.* **61,** 81 (1986).
58. K. KODAMA AND G. MUTO, *J. Solid State Chem.* **17,** 61 (1976).
59. K. KODAMA AND G. MUTO, *J. Solid State Chem.* **19,** 35 (1976).
60. W. L. ROTH, *J. Solid State Chem.* **4,** 60 (1972).
61. W. H. BAUER *in* "Structure and Bonding in Crystals" (M. O'Keeffe and A. Navrotsky, Eds.), pp. 31–52, Academic Press, New York (1981).
62. J. M. P. J. VERSTEGEN AND A. L. N. STEVELS, *J. Lumin.* **9,** 406 (1974).
63. N. IYI, Z. INOUE, AND S. KIMURA, *J. Solid State Chem.* **61,** 236 (1986).
64. W. A. ENGLAND, A. J. JACOBSON, AND B. C. TOFIELD, *Solid State Ionics* **6,** 21 (1982).
65. G. COLLIN, R. COMES, J. P. BOILOT, AND PH. COLOMBAN, *Solid State Ionics* **1,** 59 (1980).
66. N. IYI, Z. INOUE, S. TAKEKAWA, AND S. KIMURA, *J. Solid State Chem.* **60,** 41 (1985).
67. N. IYI, Y. BANDO, S. TAKEKAWA, Y. KITAMI, AND S. KIMURA, *J. Solid State Chem.* **64,** 220 (1986).
68. A. KAHN AND J. THERY, *J. Solid State Chem.* **64,** 102 (1986).
69. N. IYI, S. TAKEKAWA, AND S. KIMURA, *J. Solid State Chem.* **59,** 250 (1985).